Journal of Applied Polymer Science

Poly(aspartic acid)–tryptophan grafted copolymer and its scale-inhibition performance

Xiaoyu Sun,[1] Junping Zhang,[1] Chengxian Yin,[2] Juantao Zhang,[2] Jiao Han[1]

[1]Department of Applied Chemistry, School of Natural and Applied Sciences, Northwestern Polytechnical University, Xi'an, Shaanxi 710129, China

[2]CNPC Tubular Goods Research Institute, Xi'an, Shaanxi, China, 710077

Correspondence to: J. Zhang (E-mail: zhangjunping@nwpu.edu.cn)

ABSTRACT: Scale deposition, which severely damages oil exploration, is a difficulty encountered in oil fields. Scale inhibitors are widely used for controlling scales. Poly(aspartic acid) (PASP) is attracting more and more attention with increasing environmental concern and discharge limitations. However, PASP's poor inhibition in a high-temperature environment markedly limits its wide use. Thus, poly(aspartic acid)–tryptophan grafted copolymer (PASPTR) was synthesized to improve the inhibition efficiency of PASP. The results show that the reactant of PASPTR has a great effect on its inhibition performance. PASPTR was found to inhibit the precipitation of $CaSO_4$ close to 90% at concentrations as low as 0.4 mg/L at 50°C. The inhibition efficiency of PASPTR against $CaCO_3$ was close to 100% with the concentration of 2 mg/L at 50°C. Scanning electron microscopy and X-ray diffraction analyses, which showed the morphological and crystal structural changes of $CaCO_3$ and $CaSO_4$ precipitation, verified the excellent inhibition performance of PASPTR. © 2015 Wiley Periodicals, Inc. J. Appl. Polym. Sci. **2015**, *132*, 42739.

KEYWORDS: addition polymerization; copolymer; grafting; oil and gas

Received 19 April 2015; accepted 15 July 2015

DOI: 10.1002/app.42739

INTRODUCTION

With the rapid development of economy, the demand for oil is also growing. However, scaling is an inevitable problem during the process of the exploitation of oilfields. Scaling affects the exploitation of oilfields dramatically because it reduces the competence of affusing, the production of oil, and even destroys the equipment because of the narrowing or plugging of wells and lines with scales.[1–3] In the oil industry, carbonates and sulfates of barium, strontium, and calcium are the most common scales. Factors that influence the formation of precipitates include sudden changes in the produced fluid conditions, such as the pressure, temperature, and pH,[4] or the mixture of two incompatible brines that contain the anions, such as carbonate, sulfate, and cations, such as calcium, barium, or magnesium.[5]

The addition of chemical inhibitors is a primary method for solving scaling problems. The scale inhibitor can affect the nucleation and crystallization rates of $CaCO_3$ or $CaSO_4$ and can induce morphological changes of the crystal shape.[6–8] As a result, it possesses an excellent scale-resisting effect even when very small concentrations are added.[9,10] There are many classes of chemicals used as scale inhibitors to prevent scale formation. Natural high polymers, such as starch and tannin, were first used as scale inhibitors. Since then, phosphorus polymer scale inhibitors, poly(carboxylic acid) scale inhibitors, sulfonic acid scale inhibitors, and environmentally friendly green scale inhibitors have been developed successively.[4] Environmentally friendly green scale inhibitors have caught more attention in recent years because of the major concern over global ecological and environmental problems.[11–13] Poly(aspartic acid) (PASP), the most promising environmentally acceptable scale inhibitor, is attracting more and more attention because of its good biodegradability, nontoxicity, chelating ability, and dispersability.[14,15] Although PASP exhibits good antiscaling performance at low temperatures, its poor inhibition in high-temperature environments markedly limits its wide uses.[16,17] So, it is a challenge for us to enlarge the application scope of PASP.

Recently, chemical modification has been proven to be an efficient way for improving the antiscaling efficiency of PASP and has received more attention. Graft copolymerization is the main method for modifying PASP because PASP has amino groups that can be grafted easily.[18] The graft copolymerization of PASP can enhance PASP's heat resistance and widen PASP's applications through the choice of various types of side chains. Studies on the graft copolymerization of melamine, glutamic acid, and 2-amino-2-methyl-1,3-propanediol onto PASP have been reported.[19–21]

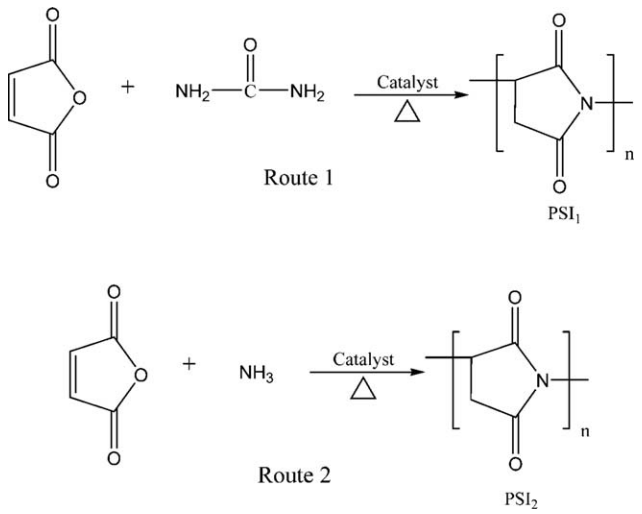

Figure 1. Synthesis routes of PSI.

In this study, tryptophan, which has good degradability, excellent solubility, and good biocompatibility as the side chain, was introduced onto PASP by graft copolymerization. Poly(aspartic acid)–tryptophan grafted copolymer (PASPTR), the product, was characterized by Fourier transform infrared spectroscopy and ^{1}H-NMR. The antiscaling behavior of the synthesized PASPTR copolymer against $CaCO_3$ and $CaSO_4$ scales in different conditions were investigated by a static scale-inhibition test. Its antiscale mechanism was investigated by means of scanning electron microscopy and X-ray diffraction. The modification approach in this study successfully enhanced the inhibition efficiency of PASP and could be a reference for future studies of the modification of PASP.

EXPERIMENTAL

Instruments and Agents

Instruments used in this research included an AVATAR-360 Fourier transform infrared spectroscope, an AVANCE 800 ^{1}H-NMR instrument, and a JSM 5600LV scanning electron microscope.

Tryptophan was purchased from Aladdin Chemical Reagent Co., Ltd. (Shanghai, People's Republic of China). Maleic anhydride (MA), urea, ammonia, sulfuric acid, phosphoric acid, ethanol, calcium chloride, sodium bicarbonate, sodium sulfate, ethylenediaminetetraacetic acid disodium salt (EDTA), and *N,N*-dimethylformamide were obtained from Sinopharm Chemical Reagent Co., Ltd. (Shanghai, People's Republic of China). All of the chemicals in this study were analytical reagent grade.

Synthesis of the PASPTR-Grafted Copolymer

Synthesis of Polysuccinimide (PSI). PSI was synthesized through two routes (see Figure 1) as follows.

Route 1. An amount of 9.8 g of MA was dissolved in appropriate water in a three-necked flask placed in an oil bath at 60°C for 40 min. After the addition of 4.2 g of urea, it was reacted for 2 h. The reaction liquid was concentrated from colorless to milky at reducing pressure at 130°C.[22] Then, 0.82 mL of mixed acids (sulfuric acid/phosphoric acid = 1 : 1) was added to the milky solution, and the polymerization was carried out at 180°C for 50 min. After the polymerization reaction, a proper amount of *N,N*-dimethylformamide was added, and the resulting solution was separated from solid by filtration. PSI (denoted as PSI_1)[23,24] was precipitated from solution by the addition of alcohol. Pure PSI was obtained after filtration and drying.

Route 2. An amount of 9.8 g of MA was dissolved in appropriate water in a three-necked flask encircled with an oil bath at 60°C for 40 min. Followed by the addition of 15 mL of ammonia, it was reacted for 2 h.[25] The reaction liquid was concentrated from colorless to yellow at 145°C for 50 min. The resulting mixture solution was separated by alcohol precipitation, filtration, and drying; this generated an intermediate PSI (denoted as PSI_2).

Synthesis of the PASPTR-Grafted Copolymer. The PASPTR-grafted copolymer was synthesized through the route shown in Figure 2.

A proper amount of tryptophan was hydrolyzed in a 2 mol/L sodium hydroxide solution. Then, the solution was divided into two parts. Two aqueous solutions containing 0.9 g of PSI_1 and PSI_2 were added and reacted for 24 h at room temperature. The solid was precipitated with the addition of alcohol. $PASPTR_1$ and $PASPTR_2$, which were orange transparent powders, were generated after filtration, washing with alcohol, and drying.

Evaluation of the Scale-Inhibition Performance of the PASPTR Copolymer Against $CaCO_3$ and $CaSO_4$ Scales

The scale-inhibition performance of the copolymers for $CaCO_3$ and $CaSO_4$ scales was investigated by static scale-inhibition tests according to the China National Standard method GB/T 16632-2008.[26] For a better evaluation of PASPTR scale inhibition, different concentrations of Ca^{2+}/HCO_3^- and Ca^{2+}/SO_4^{2-} were

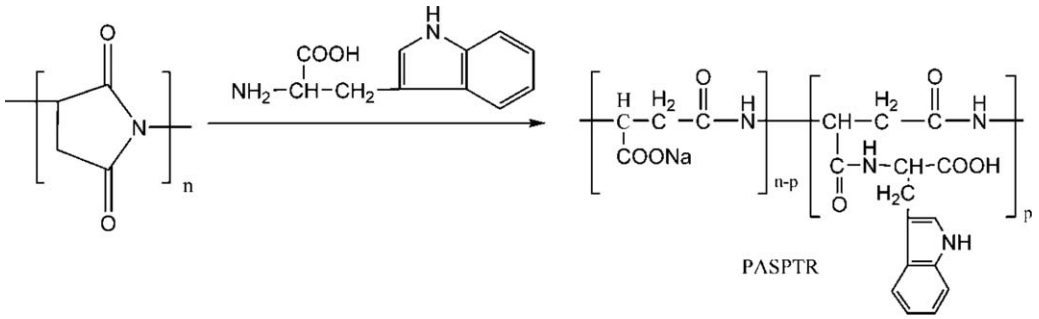

Figure 2. Synthesis route of the PASPTR graft copolymer.

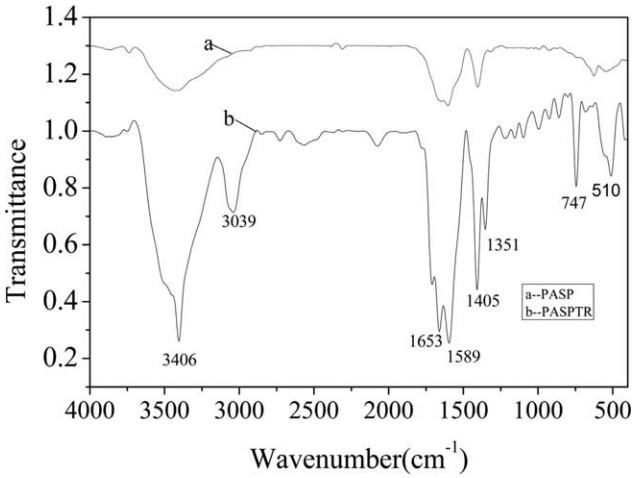

Figure 3. Fourier transform infrared spectra of PASP and PASPTR.

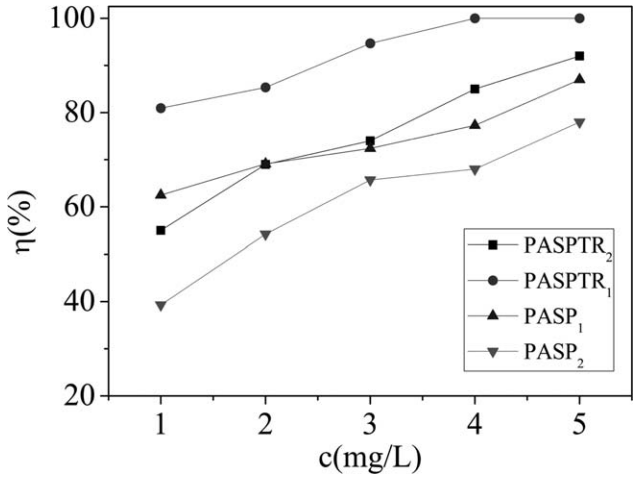

Figure 5. Influence of the reactants on the inhibition efficiency of PASP and PASPTR against the $CaCO_3$ scale (temperature = 80°C, time = 8 h; DMSO = dimethyl sulfoxide).

chosen according to the solubility of $CaCO_3$ and $CaSO_4$. For $CaCO_3$, the aqueous solution contained 250 mg/L Ca^{2+} and 250 mg/L HCO_3^-. Because the solubility of $CaSO_4$ was higher than that of $CaCO_3$, its aqueous solution contained 1500 mg/L Ca^{2+} and 3000 mg/L SO_4^{2-}.[27] In a 250-mL volumetric flask, the scale inhibitor solution was added to a Ca^{2+} stock solution followed by the dropping of bicarbonate or sulfate stock solution. The solution was allowed to react at 80°C for 8 h and was filtered after cooling. The remaining cations in the supernatant were measured by titration. The scale-inhibition efficiency of the PASPTR copolymer was calculated via eq. (1):

$$\eta = \frac{V_1 - V_2}{V_2 - V_0} \times 100\% \quad (1)$$

where V_0 and V_1 are the volumes of EDTA consumed by a certain amount of cations in the absence and presence, respectively, of scale inhibitor in the to-be-tested solution and V_2 is the volume of EDTA consumed by all of the cations in the to-be-tested solution.

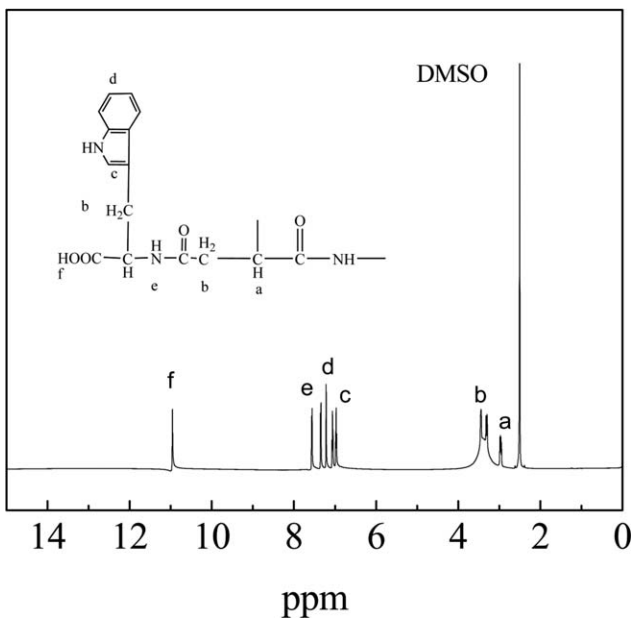

Figure 4. ^{1}H-NMR spectra of PASPTR.

RESULTS AND DISCUSSION

Fourier Transform Infrared Analysis of the Synthesized Products

Figure 3 shows the Fourier transform infrared spectra of PASP and PASPTR. Peaks at 3039 and 747 cm^{-1} were the stretching vibrations and deformation vibrations, respectively, of the C—H bonds in the benzene rings [Figure 3(b)]. The peak at 1653 cm^{-1} was the characteristic adsorption peak of C=O bond stretching vibrations.[29] The peak at 1351 cm^{-1} was the symmetric stretching peak of the COO—. Thus, we inferred that the PASPTR copolymer was successfully synthesized.

^{1}H-NMR Analysis of Synthetic Products

To confirm the structure of PASPTR, ^{1}H-NMR was carried out. The ^{1}H-NMR spectrum of PASPTR is shown in Figure 4. The 3.297–3.427-ppm NMR signals were assigned to —CH_2—. The 2.947-ppm NMR signal indicated —CH—. Signals of —COOH— were observed at 10.973 ppm. The 6.974-ppm NMR signal stood for =CH—. The 7.208–7.404-ppm NMR signals represented the existence of benzene. The 7.552-ppm NMR signals were attributed to —CO—NH—. Therefore, it was confirmed that the PASPTR with expected structure was synthesized successfully.[21,29,30]

Inhibition Efficiency of PASPTR Against $CaCO_3$

Influence of the Reactants and Concentration on the Inhibition Efficiency of PASPTR Against $CaCO_3$ Scales. Figure 5 shows the scale-inhibition test results of PASPTR and PASP synthesized from different PSIs. Compared with PASP, PASPTR showed a better scale-inhibition performance. The scale-inhibition efficiency of PASPTR was 20% greater than that of PASP when the addition concentration was 4 mg/L. $PASPTR_1$ and $PASP_1$, which were synthesized from PSI_1, showed better inhibition performance than $PASPTR_2$ and $PASP_2$ synthesized from PSI_2. The scale-inhibition efficiency of $PASPTR_1$ was close to 100%, whereas the scale-inhibition efficiency of $PASPTR_2$

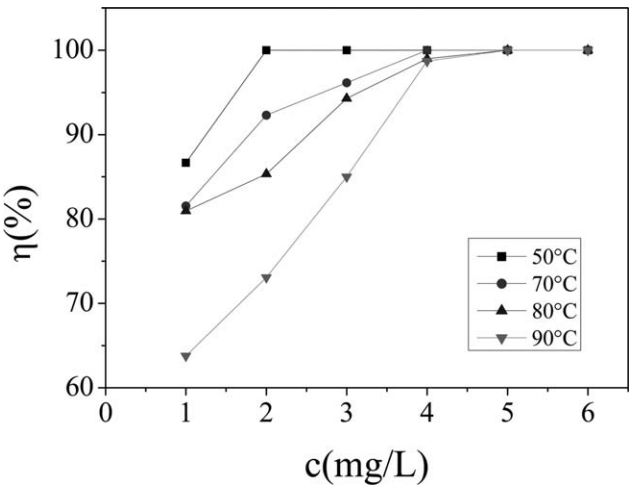

Figure 6. Influence of the concentration of PASPTR on the inhibition efficiency against the $CaCO_3$ scale at different temperatures (time = 8 h).

was about 90% when the addition concentration was 4 mg/L. $PASP_2$ showed the lowest scale-inhibition efficiency in these four compounds. The scale-inhibition efficiency of $PASPTR_1$ increased with increasing concentration in the range 1–4 mg/L and then remained stable. The scale-inhibition efficiencies of $PASPTR_2$, $PASP_1$ and $PASP_2$ increased with increasing concentration in the range 1–5 mg/L. The scale-inhibition efficiency of the four compounds followed the order

$$PASPTR_1 > PASPTR_2 > PASP_1 > PASP_2$$

This indicated that the reactants had a great effect on the inhibition efficiency of PASP and PASPTR. $PASPTR_1$ and $PASP_1$, which were synthesized from PSI_1 (the reaction product of MA and urea), had better inhibition efficiencies than the $PASPTR_2$ and $PASP_2$ synthesized from PSI_2 (the reaction product of MA and ammonia).

On the basis of the test results, $PASPTR_1$ (abbreviated as PASPTR) was chosen in the following tests.

Influence of the Temperature and Inhibitor Concentration on the Inhibition Performance of PASPTR Against $CaCO_3$ Scales. Figure 6 represents the effect of the temperature on the scale-inhibition efficiency of PASPTR against $CaCO_3$. The inhibition efficiency of PASPTR against $CaCO_3$ scales decreased slightly with increasing temperature, and $CaCO_3$ scales could be totally prevented with 5 mg/L PASPTR when the temperature reached 90°C. This indicated that the bonds between the PASPTR copolymer and Ca^{2+} were very stable. The scale-inhibition efficiency of PASPTR was 96.36% at an inhibitor concentration of 2 mg/L at 50°C. The adsorption ability and the complexion ability of the copolymer for Ca^{2+} were strengthened when the side chains with functional groups were introduced onto it; this changed calcite to vaterite and reduced the rate of nucleation and crystal growth. We inferred that the side chain with functional groups on the PASPTR copolymer enabled the inhibitor with good thermal tolerance.

Influence of the Reaction Time on the Inhibition Efficiency of PASPTR Against $CaCO_3$ Scales. PASPTR had more effective groups than PASP, and these groups had many lone-pair electrons; this increased PASPTR's activity and made it strongly chelate with Ca^{2+} to form a stable chelate compound. As a result, PASPTR retained its stable inhibition efficiency with the elongation of the reaction time. Just as Figure 7 shows, the inhibition efficiency of PASPTR against $CaCO_3$ scales at 50°C still exceeded 80% after 60 h of reaction time. This long-time stable characteristic indicated that PASPTR was an excellent scale inhibitor compared to the other inhibitors,[31–35] and this should make PASPTR be used more widely.

Influence of the Molar Ratio of Ca^{2+} to HCO_3^- on the Inhibition Efficiency of PASPTR Against $CaCO_3$ Scales. Figure 8 shows that the scale-inhibition efficiency of PASPTR against $CaCO_3$ scales was greatly affected by the molar ratio of Ca^{2+} to HCO_3^-. With other conditions remaining unchanged, the scale-inhibition efficiency of PASPTR decreased with increasing HCO_3^-. At higher Ca^{2+}/HCO_3^- molar ratios (ratio = 1.5), 2 mg/L PASPTR could totally inhibit the deposition of $CaCO_3$.

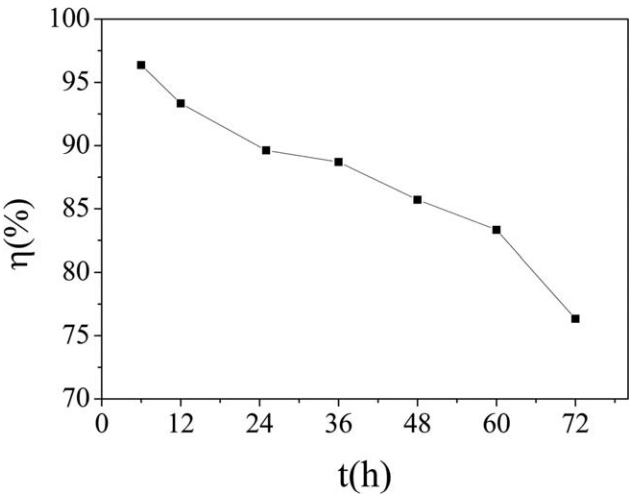

Figure 7. Influence of the reaction time on the inhibition efficiency of PASPTR against the $CaCO_3$ scale (PASPTR concentration = 4 mg/L, temperature = 80°C).

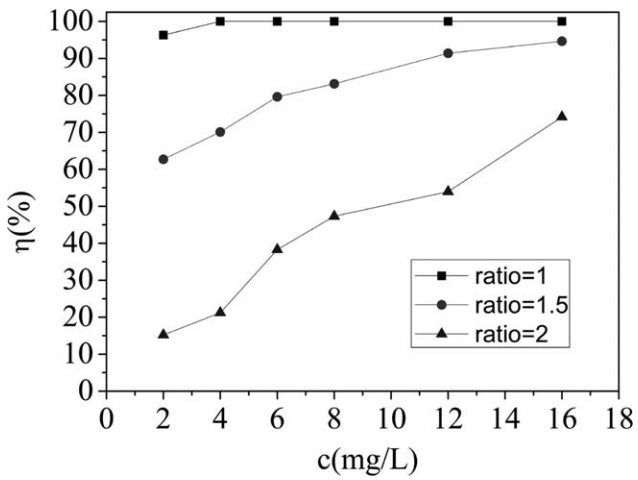

Figure 8. Influence of the Ca^{2+}/HCO_3^- molar ratio on the inhibition efficiency of PASPTR against the $CaCO_3$ scale (temperature = 80°C, time = 8 h).

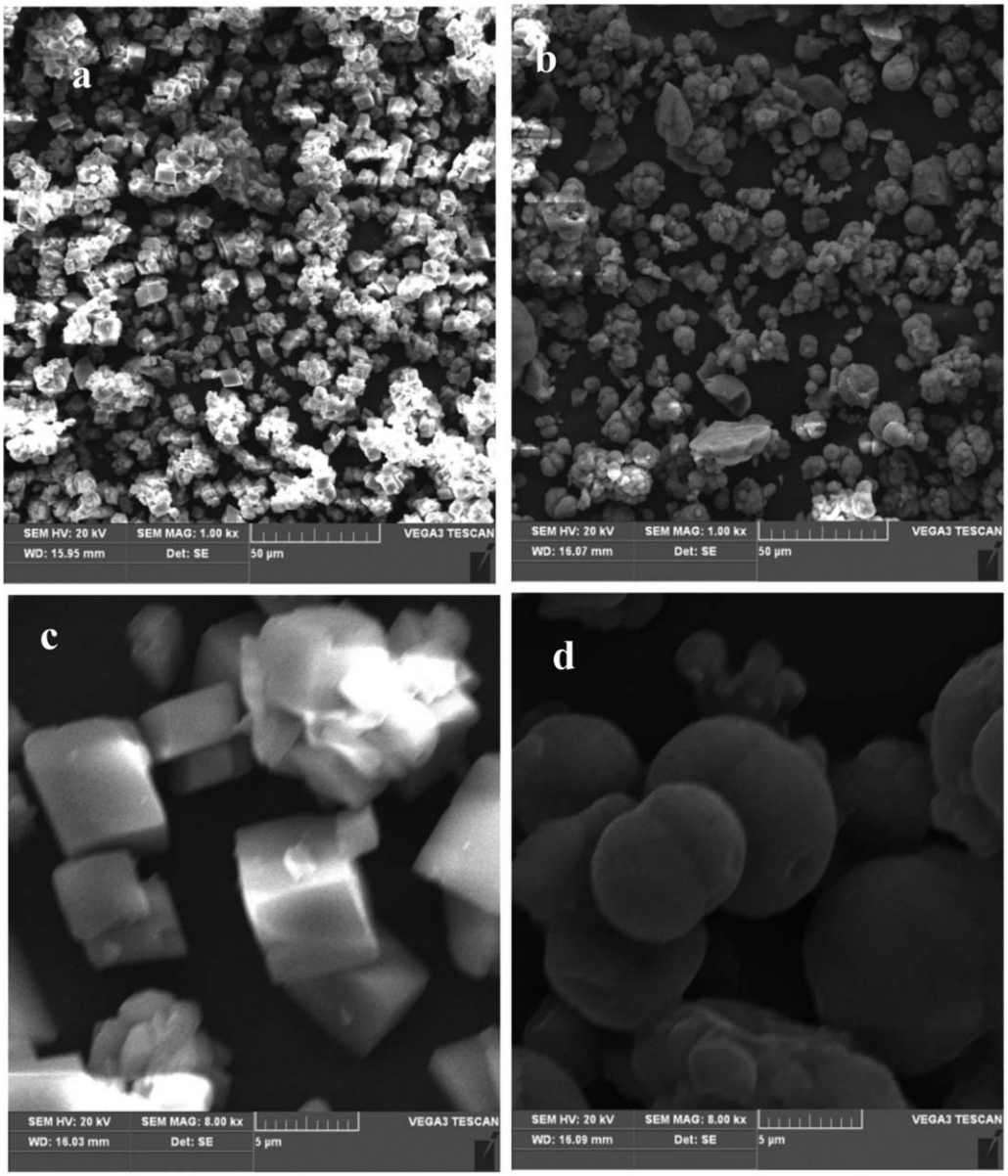

Figure 9. Scanning electron microscopy images of $CaCO_3$ powder deposits (a,c) in the absence of PASPTR inhibitor and (b,d) in the presence of PASPTR inhibitor [(a,b) 1000× and (c,d) 8000× magnification].

With a decrease in the molar ratio (ratio = 1.0), a small amount of PASPTR could not supply enough functional groups to chelate with Ca^{2+}; this led to a lower inhibition efficiency. However, the $CaCO_3$ scale could also be significantly inhibited at higher PASPTR concentrations. When the molar ratio reached a certain value (ratio = 0.5), the scale-inhibition efficiency of PASPTR decreased rapidly. At low Ca^{2+}/HCO_3^- molar ratios, the $CaCO_3$ scale crystals grew rapidly. Under these circumstances, even much higher concentrations of PASPTR could not effectively prevent the scaling of $CaCO_3$.

Effect of PASPTR on the Crystal Morphology of $CaCO_3$. Figure 9 shows the effect of the PASPTR copolymer on the morphologies of $CaCO_3$. The $CaCO_3$ deposits that formed in the absence of PASPTR were dense and had a regular shape and glossy surface.[36] In contrast, flowerlike and cascadelike agglomerated $CaCO_3$ deposits were obtained because of the blocked growth of $CaCO_3$ crystals when PASPTR was introduced into the $Ca(HCO_3)_2$ solution. Groups in the PASPTR molecules, such as carboxyls, could effectively be adsorbed at the surface of calcite and break the structure of calcite; this changed the structure and properties of the scales. Consequently, the scales were hardly attached to the pipe surface and could be easily washed away by flowing water.

X-ray Diffraction Analysis of the $CaCO_3$ Powder. As shown in Figure 10, in comparison with spectrum a, spectrum b showed diffraction peaks of 23.2 and 31.9°, which were significantly enhanced, and diffraction peaks of 29.5, 36.2, 39.6, 43.4, and 47.7°, which were obviously reduced. These changes indicated

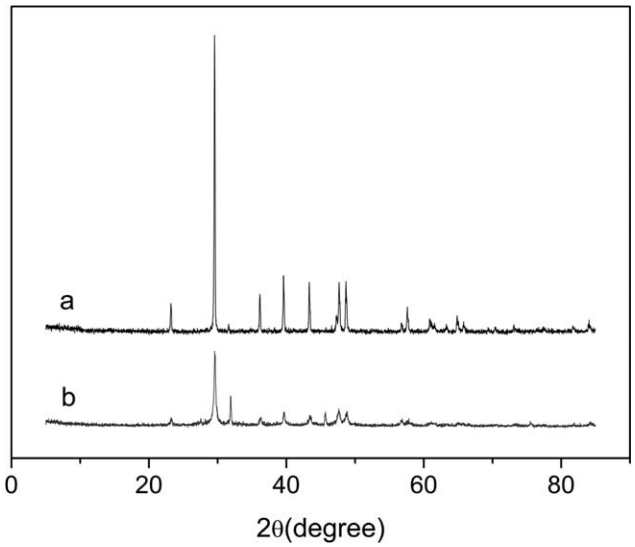

Figure 10. X-ray diffraction spectra of the $CaCO_3$ crystal (a) in the absence of PASPTR and (b) in the presence of PASPTR.

that the $CaCO_3$ crystals formed in the solution with PASPTR had significantly different crystal habits and structures compared with the bland sample. Thus, PASPTR contributed to the damage and distortion of $CaCO_3$ crystals.

Inhibition Efficiency of PASPTR Against $CaSO_4$ Scales

Influence of the Reaction Temperature and Concentration of PASPTR on the Inhibition Efficiency Against $CaSO_4$ Scales. Figure 11 shows the relationship between the inhibition efficiency and the concentration of PASPTR at different temperatures. This indicated that PASPTR had superior inhibition performance for $CaSO_4$ scales at lower temperatures. The inhibition efficiency of PASPTR for $CaSO_4$ scales was close to 100% at a concentration of only 0.6 mg/L at 50 and 70°C. At lower temperatures, PASPTR had better complexion ability for Ca^{2+} and could greatly reduce the rate of nucleation growth of $CaSO_4$. However, PASPTR had a poor inhibition efficiency against $CaSO_4$ at higher temperatures because the rate of scale

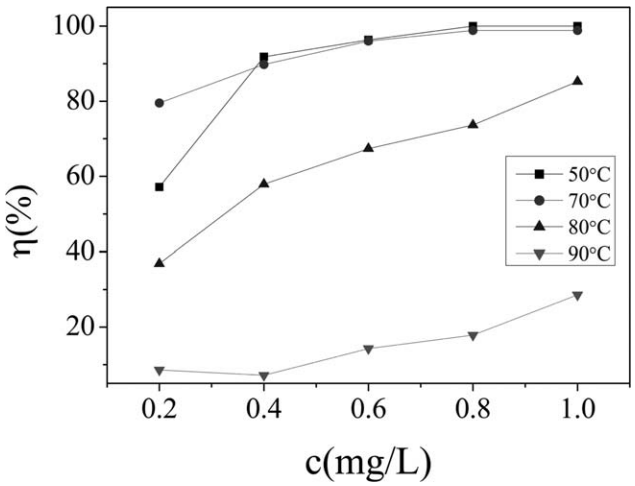

Figure 11. Influence of the concentration of PASPTR on the inhibition efficiency against the $CaSO_4$ scale at different temperatures (time = 8 h).

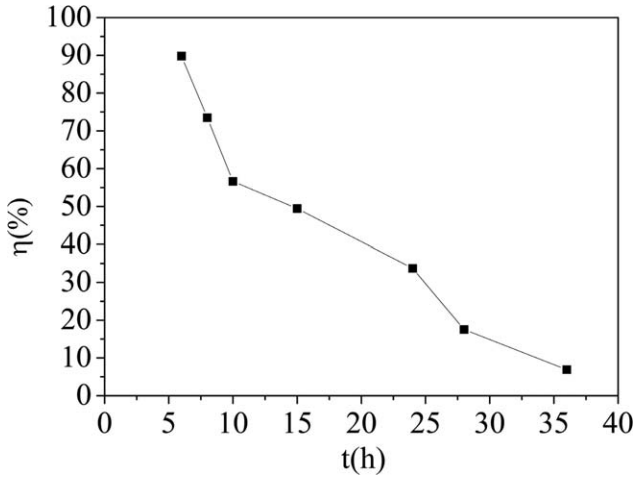

Figure 12. Influence of the reaction time on the inhibition efficiency of PASPTR against the $CaSO_4$ scale (temperature = 70°C, concentration = 0.4 ppm).

formation exceeded the rate of chelate formation in high-temperature environments.

Influence of the Reaction Time on the Inhibition Efficiency of PASPTR Against $CaSO_4$ Scales. Figure 12 shows the changes in the inhibition efficiency of PASPTR against $CaSO_4$ scales with the reaction time. This showed that the inhibition efficiency of PASPTR declined rapidly with the heating time. In this system, the electrostatic interaction between Ca^{2+} and SO_4^{2-} was much stronger than that between PASPTR and Ca^{2+}; this led to $CaSO_4$ scales being formed more easily with increasing reaction time. The inhibition efficiency of PASPTR against $CaSO_4$ was nearly 90% after 6 h of reaction, and it decreased to 6.9% after 36 h.

Effect of PASPTR on the Crystal Morphology of $CaSO_4$. Figure 13 is the scanning electron microscope photographs of $CaSO_4$ crystals in the absence and presence of PASPTR. $CaSO_4$ crystals in the absence of PASPTR were fibrous and compact [Figure 13(a)]. The shapes of the $CaSO_4$ crystals changed completely in the presence of PASPTR to crystal shards and had irregular shape [Figure 13(b)]. PASPTR could chelate with Ca^{2+} and doted doping crystal lattice; this could inhibit the normal growth of $CaSO_4$ crystals as an array of a crystal lattice.[37] Therefore, PASPTR could prevent scales from growing and adhering to equipment surfaces for scale-inhibition purposes.

X-ray Powder Diffraction Analysis of the $CaSO_4$ Powder. As shown in Figure 14, in comparison with spectrum a, spectrum b showed diffraction peaks of 31.3, 31.9, 33.6, and 43.6°, which were significantly enhanced, and diffraction peaks of 11.8, 23.7, 35.8, 48.2, 50.7, and 75.3°, which were obviously reduced. These changes indicated that $CaSO_4$ crystals formed in the solution with PASPTR had significantly different crystal habits and structures compared with the bland sample. Thus, PASPTR contributed to the damage and distortion of $CaSO_4$ crystals.

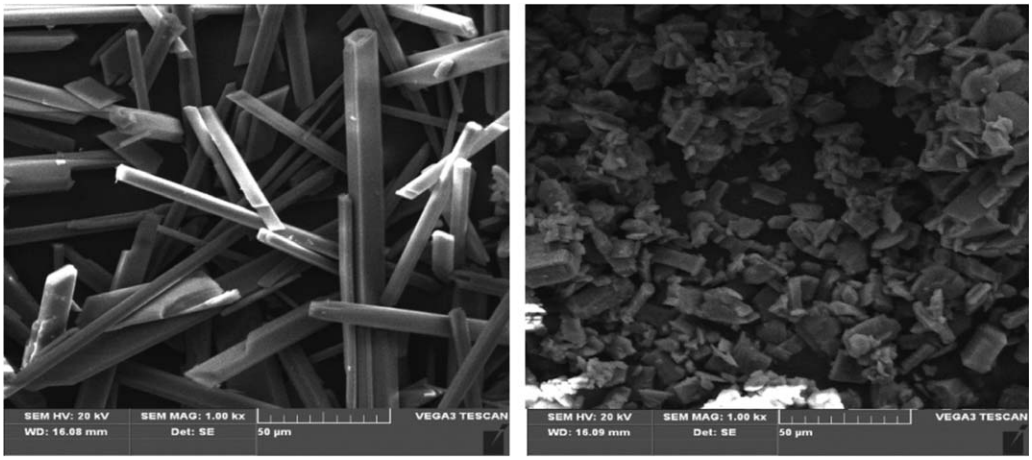

Figure 13. Scanning electron microscopy images of the $CaSO_4$ powder deposits (a) in the absence of PASPTR inhibitor and (b) in the presence of PASPTR inhibitor.

CONCLUSIONS

PASPTR, a novel graft copolymer, was synthesized successfully, and its scale-inhibition performance against $CaCO_3$ and $CaSO_4$ was evaluated by a static scale-inhibition method. The results indicate that PASPTR had excellent inhibition ability against $CaSO_4$ and $CaCO_3$ scales. The PASPTR reactant had great effect on its inhibition performance. PASPTR, synthesized with MA, urea, and tryptophan, showed better inhibition performance than that synthesized from MA, ammonia, and tryptophan. The inhibition efficiencies of PASPTR against $CaCO_3$ and $CaSO_4$ scales were 96 and 90%, respectively, with 4 mg/L at 80°C and 0.4 mg/L at 70°C, respectively. Meanwhile, the inhibition efficiency of PASPTR against $CaCO_3$ scales still exceeded 80% after 60 h of reaction, and the inhibition efficiency of PASPTR against $CaSO_4$ scales exceeded 60% after 10 h of reaction. This indicated that PASPTR had good chemical stability and thermal tolerance at elevated temperatures. PASPTR had great adsorption properties and lattice distortion properties; this changed the original scale crystals into loose and irregular crystals.

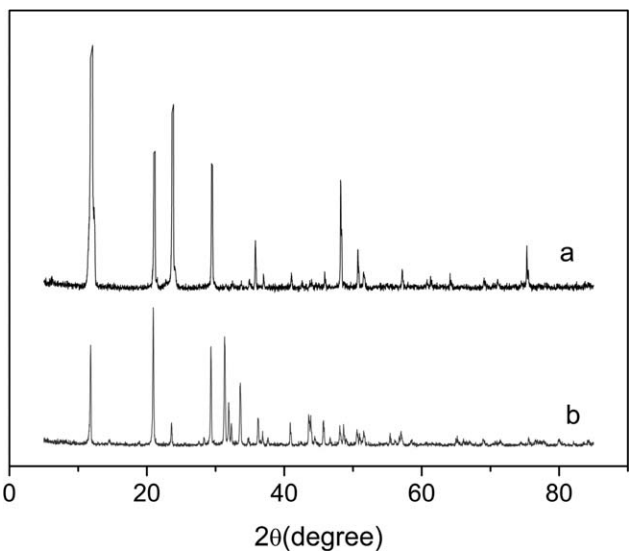

Figure 14. X-ray diffraction spectra of the $CaSO_4$ crystal (a) in the absence of PASPTR and (b) in the presence of PASPTR.

REFERENCES

1. Lin, Y. P.; Singer, P. C. *Water Res.* **2005**, *39*, 4835.
2. Koutsoukos, P. G.; Kontoyannis, C. G. *J. Cryst. Growth* **1984**, *69*, 367.
3. Belarbi, Z.; Gamby, J.; Makhloufi, L. *J. Cryst. Growth* **2014**, *386*, 208.
4. Wang, C.; Li, S. P.; Li, T. D. *Desalination* **2009**, *249*, 1.
5. Hasson, D.; Shemer, H.; Sher, A. *Ind. Eng. Chem. Res.* **2011**, *50*, 7601.
6. Lattemann, S.; Hopner, T. *Desalination* **2008**, *220*, 1.
7. Reddy, M. M.; Hoch, A. R. *J. Colloid Interface Sci.* **2001**, *235*, 365.
8. Tang, Y.; Yang, W.; Yin, X.; Liu, Y. *Desalination* **2008**, *228*, 55.
9. Qiang, X. H.; Sheng, Z. H.; Zhang, H. *Desalination* **2013**, *309*, 237.
10. Touir, R.; Dkhireche, N.; Touhami, M. E. *Mater. Chem. Phys.* **2010**, *122*, 1.
11. Martinod, A.; Nevillea, A.; Euvrad, M.; Sorbie, K. *Chem. Eng. Sci.* **2009**, *64*, 2413.
12. Martinod, A.; Euvrard, M.; Foissy, A.; Neville, A. *Desalination* **2008**, *220*, 345.
13. Liu, W. B.; Dong, F. T.; Li, F. T.; Hui, F.; Lédion, J. *Desalination* **2012**, *304*, 1.
14. Liu, Z. Y.; Sun, Y. H.; Zhou, X. H.; Wu, T.; Tian, Y.; Wang, Y. Z. *J. Environ. Sci.* **2011**, *23*, 153.
15. Idomura, Y.; Tokuda, S.; Wakatani, M.; Okaji, M.; Yamada, N.; Kato, H.; Nara, K.; Hasson, D.; Bramson, D.; Limoni-Relis, B.; Semiat, R. *Desalination* **1997**, *108*, 67.
16. Tang, S.; Fu, S. L.; Emmons, D. H. U.S. Pat. 6,022,401 (**2000**).

17. Kunjapur, M. M.; Hartt, W. H.; Smith, S. W. *Corros. Sci.* **1987**, *43*, 674.
18. Sikes, C.; Ringsdorf, L.; Swift, G. PCT Pat. Appl. WO2002062871 (**2002**).
19. Nakato, T.; Tomida, M.; Suwa, M.; Morishima, Y.; Kusuno, A.; Kakuchi, T. *Polym. Bull.* **2000**, *44*, 385.
20. Sikes, C. S.; Wheeler, A. P. U.S. Pat. 4,534,881 (**1985**).
21. Xu, Y.; Zhao, L. L.; Wang, L. N.; Xu, S. Y.; Cui, Y. C. *Desalination* **2012**, *286*, 285.
22. He, H. J.; Xu, C. X.; Wang, Y. H.; Zhan, S. X.; Ma, Y. Y.; Yang, Y. P. *Ind. Water Treat.* **2003**, *23*, 33.
23. Morad, M. S.; Kamal, A. M.; Dean, E. *Corros. Sci.* **2006**, *48*, 3398.
24. Ketrane, R.; Saidani, B.; Gil, O.; Leleyter, L.; Baraud, F. *Desalination* **2009**, *249*, 1397.
25. Kim, J. G.; Lee, J. H.; Seo, S. D.; Yu, Y. I. PCT Pat. Appl. WO2008038874 (**2008**).
26. Pairat, R.; Sumeath, C.; Browning, F. H.; Fogler, H. S. *Langmuir 1997*, 13, 1791.
27. Li, H. S.; Li, W.; Qi, X. *J. Desalination* **2007**, *214*, 193.
28. Touir, R.; Cenoui, M.; El Bakri, M.; Touhami, M. E. *Corros. Sci.* **2008**, *50*, 1530.
29. Zhang, B.; Zhou, D. P.; Lv, X. G.; Xu, Y.; Cui, Y. C. *Desalination* **2013**, *327*, 32.
30. Feng, J. Y.; Gao, L. J.; Wen, R. Z.; Deng, Y. Y.; Wu, X. J.; Deng, S. L. *Desalination* **2014**, *345*, 72.
31. Rahman, F. *Desalination* **2013**, *319*, 79.
32. Touir, R.; Dkhireche, N.; Touhami, M. E.; Bakri, M. E.; Rochdi, A. H.; Belakhmima, R. A. *J. Saudi Chem. Soc.* **2011**, *20*, 416.
33. Kuma, T.; Vishwanatham, S.; Kundu, S. S. *J. Pet. Sci. Eng.* **2010**, *71*, 1.
34. Tang, J. S.; Fu, S. L.; Emmons, D. H. U.S. Pat. 6,024,401 (**2000**).
35. Wang, R.; Zhang, Q.; Ding, J. *Ind. Eng. Chem. Res.* **2001**, *18*, 79.
36. Liu, D.; Dong, W. B.; Li, F. T.; Hui, F.; Lédion, J. *Desalination* **2012**, *304*, 1.
37. Yang, Q. F.; Liu, Y. Q.; Gu, A. Z.; Ding, J.; Shen, Z. Q. *J. Colloid Interface Sci.* **2001**, *240*, 608.